RSC Pharmaceutics

ROYAL SOCIETY OF CHEMISTRY

COMMUNICATION

View Article Online
View Journal | View Issue

Cite this: *RSC Pharm.*, 2025, **2**, 1431

Received 30th March 2025,
Accepted 21st July 2025

DOI: 10.1039/d5pm00088b

rsc.li/RSCPharma

Reversibility of FUS-aided blood–tumor barrier opening for the delivery of therapeutics

Céline Chevaleyre,[a] Sophie Tran,[a] Mylène Richard,[a] Laurène Jourdain,[a] Dimitri Kereselidze,[a] Benoit Jego,[a] Erwan Selingue,[b] Benoit Larrat,[b] Sébastien Mériaux,[b] Nicolas Tournier,[a] Anthony Novell*[a] and Charles Truillet *[a]

Focused ultrasound (FUS) offers reversible disruption of the blood–brain barrier (BBB), which enables drug delivery to the brain. However, the impact of FUS on the blood–tumor barrier (BTB) remains largely misunderstood. The reversibility of FUS-induced BTB opening was monitored using PET imaging in a glioblastoma model. C57Bl/6 mice with bilateral GL261-GFP tumors received FUS specifically targeting the right hemisphere, followed by injections of the BBB permeability marker [^{18}F]fluoro-deoxysorbitol (183 Da) or the radiolabeled antibody [^{18}F]avelumab (150 kDa). PET acquisitions were performed at 1 h, 24 h and 72 h post-FUS. The uptake of [^{18}F]avelumab and [^{18}F]fluoro-deoxysorbitol increased immediately after FUS. At 24 h post-FUS, BTB permeability returned to the baseline, as evidenced by consistent [^{18}F]avelumab distribution volumes (V_T) between tumors. By 72 h, increased radiotracer uptake indicated tumor progression. These findings highlight the potential of FUS to enhance the delivery of therapeutics to the brain while preserving BTB integrity over time.

Introduction

The vasculature within gliomas is dysfunctional, comprising a mix of continuous capillaries, fenestrated capillaries, and capillaries with inter-endothelial gaps.[1] This distinct vascular network is referred to as the blood–tumor barrier (BTB), a critical component of glioma biology. Despite its enhanced permeability compared to the blood–brain barrier (BBB), a highly selective barrier composed of endothelial cells, pericytes, and astrocytes, the BTB remains a significant obstacle to effective drug delivery to glioma tissues. While the BBB protects the brain by limiting substance passage from the bloodstream, the BTB forms when brain tumors disrupt the BBB, creating a more permeable but heterogeneous vasculature. This results in abnormal blood vessels, damaged endothelial cells, and disrupted tight junctions, causing uneven drug delivery and reduced treatment efficacy within tumors. Despite being leakier than the BBB, the BTB still hinders many chemotherapeutic agents, with permeability varying across tumor types and regions.[2] This variability in drug delivery poses a major challenge for the consistency of therapeutic efficacy in patients.[3]

One promising technique to address this issue is focused ultrasound (FUS)-mediated brain barrier opening.[4] This non-invasive approach has been extensively studied and applied to enhance the delivery of chemotherapy and immunotherapy directly to glioma tissues. FUS applied to intravenously administered microbubbles temporarily disrupts the BBB and BTB, allowing greater penetration of therapeutic agents, and could boost antitumor immune responses in patients with high-grade gliomas.[5] Remarkably, the safety of this method has been widely demonstrated in humans,[6] making it an attractive option for glioma treatment.

While FUS-aided BBB disruption has been widely studied, including by our research team,[7–9] the specific effects of FUS on the BTB remain underexplored. In particular, the transient nature of FUS-mediated BTB disruption needs further investigation, given the delicate structure of the BTB and its link with tumor progression.

In this study, we aim to quantitatively investigate the effects of FUS on the BTB by employing positron emission tomography (PET). The BTB's status was monitored post-FUS by tracking the passage of both a large biomolecule, [^{18}F]avelumab (150 kDa), and a small molecule [^{18}F]fluoro-deoxysorbitol ([^{18}F]FDS, 183 Da), a marker of BBB permeability, across the barrier at selected time points.

Materials and methods

The detailed methods are available in the SI.

[a]*Paris-Saclay University, CEA, CNRS, Inserm, BioMaps, Service Hospitalier Frédéric Joliot, SHFJ, 4 place du Général Leclerc, 91401 Orsay, France.*
E-mail: celine.chevaleyre@universite-paris-saclay.fr, anthony.novell@universite-paris-saclay.fr, charles.truillet@cea.fr
[b]*Paris-Saclay University, CEA, CNRS, NeuroSpin/BAOBAB, Centre d'études de Saclay, Bâtiment 145, 91191 Gif sur Yvette, France*

GL261-GFP orthotopic model

Eight C57BL/6 mice were orthotopically implanted with the syngeneic cell line GL261-GFP (obtained from the Institute of Neurophysiopathology, Aix-Marseille University), with 5×10^4 cells in 1 μL PBS injected into both striata. With bregma as the origin, implantation coordinates were $X = 0$ mm, $Y = \pm 2$ mm, and $Z = -3$ mm. We achieved a 100% tumor formation success rate post-implantation, confirmed by MRI.

MRI

Fourteen days after GL261-GFP implantation, *T*1-weighted contrast-enhanced MRI scans were acquired with a 7 T/90 mm borehole MRI scanner (Pharmascan scanner, Bruker). A gadolinium-based contrast agent (Dotarem®, 1 nm diameter, 100 μL per animal) was intravenously injected *via* a catheter before acquiring the *T*1-weighted images.

Radiolabeling of avelumab

Radiofluorination of [^{18}F]avelumab was carried out in two steps. The prosthetic group [^{18}F]FPyNHS was first synthesized on an AllInOne automate[10] and then conjugated to avelumab *via* the amino groups of lysine residues.

[^{18}F]FDS production

[^{18}F]FDS was obtained according to a previous protocol.[11]

Blood–tumor barrier disruption

The FUS protocol was similar to that used in ref. 8, except that ultrasound was transmitted in only one hemisphere. This FUS condition has already been demonstrated to be safe.[12] Briefly, 50 μL of SonoVue microbubbles (Bracco) were intravenously administered before sonication. A large mechanical scan of 6 mm × 6 mm was performed over the animal's head, but ultrasound (1.5 MHz, 420 kPa) was transmitted only over a 6 mm × 3.6 mm area corresponding to the right hemisphere only, enabling BBB disruption to the full depth of the brain hemisphere. Acoustic pressure was set to 0 kPa over the rest of the trajectory, allowing the left hemisphere to remain as a control. The trajectory was repeated for a total of 2 min.

microPET/CT imaging

On day 15 after GL261-GFP implantation, a 60 min dynamic PET scan was performed after the injection of [^{18}F]avelumab (6.7 ± 4.2 MBq, 75 ± 4 μg, $n = 4$) under the camera. A 30 min dynamic PET scan was performed after the injection of [^{18}F]avelumab (6.7 ± 1.7 MBq, $n = 4$) under the camera. The radioligand injection was performed immediately after the end of the FUS protocol: 2.9 ± 0.1 min for [^{18}F]avelumab and 2.9 ± 0.0 min for [^{18}F]FDS. Subsequent [^{18}F]avelumab PET scans were performed at 24 h (9.5 ± 4.5 MBq, 80 ± 6 μg, $n = 4$) and 72 h post-FUS (3.7 ± 1.8 MBq, 62 ± 2 μg, $n = 4$). Subsequent [^{18}F]FDS PET scans were performed at 24 h (7.7 ± 4.2 MBq, $n = 4$) and 72 h post-FUS (10.2 ± 1.3 MBq, $n = 4$).

Immunofluorescence

After the last imaging session, mice were sacrificed and perfused with saline solution. Their brains were collected, immersed in isopentane, and frozen in liquid nitrogen. A set of fixed, frozen brain sections (10 μm) were incubated with anti-GFP AF488 and rat anti-mouse CD31 antibodies. The slides were then incubated with an anti-rat AF546-conjugated secondary antibody and an AF647-conjugated goat anti-human secondary antibody to stain the injected avelumab. Immunofluorescent sections were scanned with an AxiObserver Z1 microscope (Zeiss).

Results

Distribution of [^{18}F]avelumab and [^{18}F]FDS following BTB disruption by FUS

As anticipated, the BTB in the GL261-GFP model showed some leakage, allowing both [^{18}F]avelumab and [^{18}F]FDS to cross into the left tumor, which did not receive FUS (Fig. 1B). After FUS treatment on the right hemisphere, [^{18}F]avelumab uptake in the right tumor was slightly higher compared to the left tumor ($AUC_{0-60\ min} = 161 \pm 9$ *versus* 143 ± 8% ID min cm^{-3}, $p < 0.01$, Fig. S7). For [^{18}F]FDS, there was no significant difference in exposure between the right and left tumors ($AUC_{0-30} = 44 \pm 3$ in the left tumor and 45 ± 2% ID min cm^{-3} in the right tumor, $p > 0.05$, Fig. S8). At 24 and 72 hours post-FUS, the left tumor, which did not receive FUS, showed higher exposure to both radioligands. This is consistent with the initial BTB status observed in the *T*1-weighted contrast-enhanced MRI, where the left tumor presented a higher volume than the right tumor (Fig. S6–8). As a consequence, the FUS-to-sham tumor ratio of [^{18}F]avelumab was greater immediately after FUS, but not at 24 and 72 hours post-FUS, where the ratio remained stable (1.25 ± 0.27 at 1 h post-FUS, *versus* 0.85 ± 0.13; $p < 0.01$ at 24 h and 0.89 ± 0.07; *p*-value = 0.04 at 72 h) (Fig. 1D and E). [^{18}F]avelumab blood pool content was significantly higher at 24 hours, which can be explained by saturation of the antigen sink between 24 h and 48 h, related to the long half-life of avelumab.

Quantifying the passage of [^{18}F]-avelumab provides insights into the BTB status

The distribution volume ($V_T = K_1/k_2$) of [^{18}F]avelumab was estimated by fitting a 1-tissue compartment model to the tumors' time–activity curves. Immediately following FUS-aided disruption, the V_T in targeted tumors increased significantly by ~50%. Interestingly, 24 hours later, the V_T in FUS-treated tumors dropped sharply, falling below the levels observed in the sham-treated tumors. At 72 hours, V_T increased in all tumors, with higher values remaining in the sham-treated tumors (Fig. 2A). No significant correlation was observed between the V_T obtained 1 h post-FUS and tumor volume determined by MRI. In contrast, a significant correlation emerged 24 hours later between V_T and the baseline BTB status (before FUS, Fig. 2B). This suggests that 24 hours post-

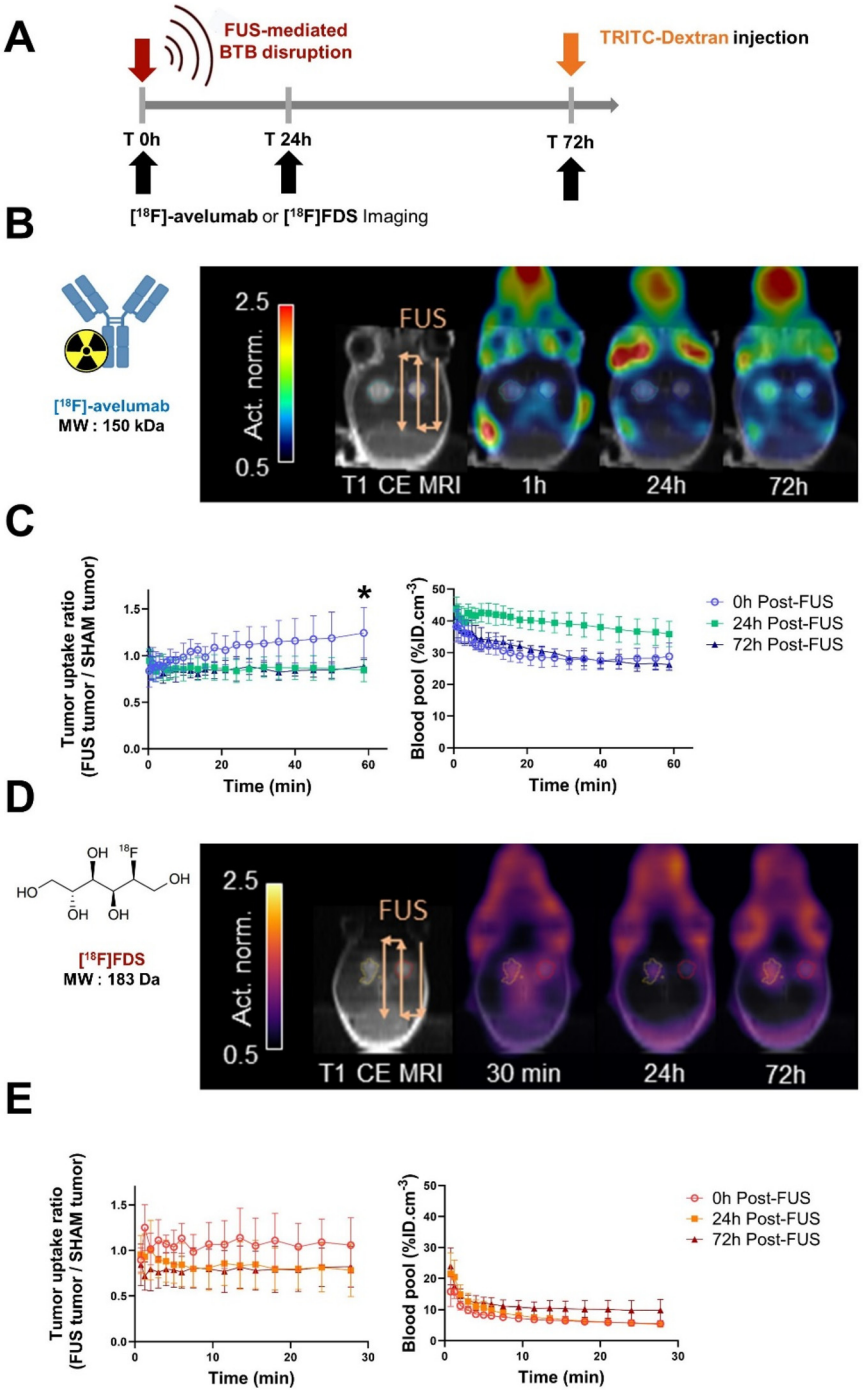

Fig. 1 Blood–tumor barrier opening by FUS and its impact on the delivery of [^{18}F]-avelumab and [^{18}F]FDS. (A) Study timeline. (B) Representative *T*1-weighted MRI with contrast enhancement and averaged PET images over the last 20 minutes of the acquisitions. [^{18}F]-avelumab was injected immediately after the FUS protocol, as well as at 24 h and 72 h post-FUS. PET images are normalized to the peak voxel value in the left tumor. (C) Tumor uptake ratios of [^{18}F]-avelumab (n = 4 mice) between the tumor with FUS-aided BTB disruption and the contralateral tumor; corresponding blood curves. (D) Representative *T*1-weighted MRI with contrast enhancement and averaged PET images over the last 10 minutes of the acquisitions. [^{18}F]FDS was injected immediately after the FUS protocol, as well as at 24 h and 72 h post-FUS. PET images are normalized to the peak voxel value in the left tumor. (E) Tumor uptake ratios of [^{18}F]FDS (n = 4 mice); corresponding blood curves. All data are represented as mean ± SD.

FUS, the observed uptake in the tumor is more closely related to the tumor burden. In contrast, the increased uptake immediately after FUS is likely due to enhanced drug entry into the tumor (Fig. S9 and 10). Immunofluorescence analysis at 72 hours post-FUS revealed that the total amount of avelumab in the FUS-treated tumor was significantly higher than in

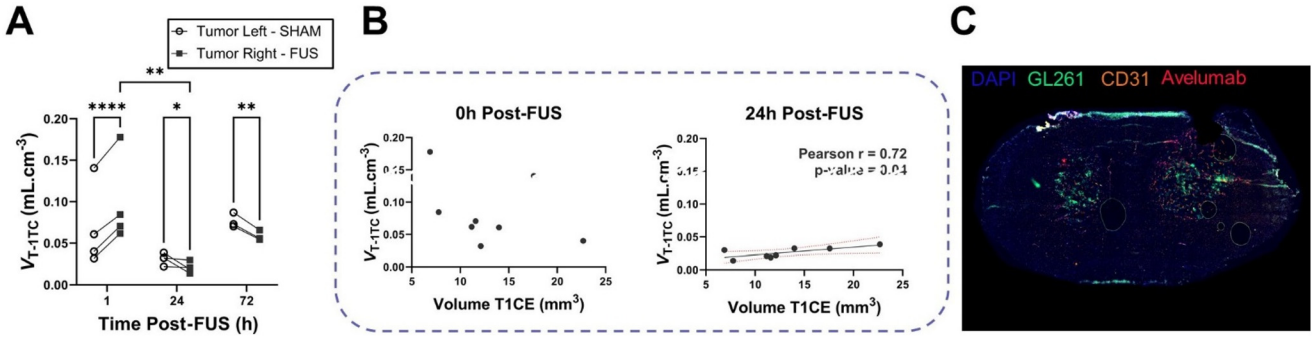

Fig. 2 [^{18}F]-avelumab distribution comparing the disrupt BTB and the sham BTB over time. (A) Distribution volumes (V_T) of [^{18}F]-avelumab estimated from fitting a 1-tissue compartment model for the FUS-exposed tumor and the contralateral tumor. (B) Correlation between the [^{18}F]-avelumab distribution volume and the volume of the initial BTB disruption determined by the *T*1-weighted MRI with gadoteric acid contrast enhancement. (C) Immunofluorescence staining of the injected avelumab (red) and the endothelial cells (orange) on a section of a mouse brain bearing two GL261-GFP tumors (green), harvested at 72 h post-injection. The immunofluorescence signal is overlaid on DAPI images (blue).

the sham tumor (Fig. 2C, with quantification in Fig. S11). This underscores the critical role of FUS in enhancing avelumab delivery in a reversible manner, compared to its natural passage through the impaired BTB.

Discussion/conclusion

It is generally accepted that BBB disruption after FUS is reversible, within 24 hours, a conclusion largely based on preclinical and clinical studies using gadolinium-based MRI contrast agents in the context of a healthy and functional BBB.[6] In clinical trials evaluating the treatment of brain tumors by FUS-enhanced delivery of therapeutics, the targeted lesions already exhibit a dysfunctional BTB that allows the diffusion of the MRI contrast agent before any FUS.[13] Given that the BTB is inherently fragile and exhibits heterogeneous vascular structures,[14] the transient nature of FUS-induced disruption required further investigation.

In a recent study, we assessed the extent and duration of BBB and BTB opening for a full IgG antibody following FUS exposure, with both being comparable.[8] However, when monitoring the kinetics of the radiolabeled antibody, we observed a progressive accumulation in the tumor beginning 48 hours post-injection, following FUS-induced BBB/BTB opening. Based on these findings, it remains unclear whether this accumulation is due to the tumor's natural progression or a prolonged effect of the FUS on the BTB.

The present study demonstrates that the delivery of [^{18}F]avelumab is facilitated by the FUS-induced BTB opening, but is less effective for [^{18}F]FDS, which can be explained by its smaller molecular weight and rapid plasma clearance compared to a full IgG such as avelumab. As vascular endothelium reclosure after FUS is progressive, the time during which paracellular passage is possible is highly dependent on the size and physicochemical properties of the therapeutic molecule under consideration.[7,15] Furthermore, it is recognized that the opening of the BBB by FUS induces inflammatory reactions and regulates the expression of certain proteins, effects that may persist for several days.[16,17] Therefore, size is an important, but not the only, parameter influencing the tumor uptake of a drug. The BTB is characterized by a decreased expression of influx and efflux transporters, accompanied by an increase in the number of caveolae and an intensification of pinocytosis.[18] Recent studies suggest that the distribution of therapeutic antibodies in brain metastases may rely more on active intracellular transport mechanisms, such as endocytosis, rather than solely on paracellular permeability.[19,20] This highlights the complex relationship between BTB dynamics and molecular size, where larger molecules like antibodies can, in some cases, achieve greater efficacy than smaller compounds. FUS may not only facilitate paracellular transport but also modulate intracellular trafficking pathways at the BTB, potentially enhancing the delivery of larger molecules. This additional layer of complexity in BTB modulation by FUS should be further explored to fully leverage its therapeutic potential for brain tumors.

However, at 24 hours post-FUS, the BTB's permeability returned to the baseline levels comparable to those obtained before FUS. By 72 hours post-FUS, the increased distribution of both [^{18}F]avelumab and [^{18}F]FDS across all tumors suggests tumor progression, consistent with the aggressive nature of the GL261-GFP glioblastoma model, with a progressive increase in BTB permeability. Additionally, quantification of the TRICT-dextran injected 72 h post-FUS showed no significant difference between the two tumors, further confirming the reversibility of the FUS-induced BTB disruption (Fig. S12). This finding underscores the need for multiple FUS sessions to optimize drug delivery, even when the BTB is already leaky, to reinforce the potential of therapeutics for improved and/or homogeneous treatment outcomes. The necessity for repeated FUS treatments may vary depending on the tumor type and its specific characteristics in clinical practice. For instance, tumors with inherently leaky BTBs might require several FUS sessions, but fewer compared to those with more intact barriers, to reach optimal drug occupancy. Personalized treatment

strategies, tailored to the individual characteristics of each patient's tumor, are likely required to maximize therapeutic efficacy. Such strategies could involve adjusting the frequency and timing of FUS sessions based on real-time monitoring of BTB permeability and tumor response.

Animals

The authors adhered to the ARRIVE guidelines. There is no fully reliable or validated alternative to animal models for reproducing the intricate complexity of the tumor microenvironment, particularly the unique vascularization seen in glioblastoma. While *in vitro* systems, such as cell lines or organoids, and *in silico* simulations enable the study of isolated mechanisms, they fall short of capturing the dynamic interplay between immune cells, metabolic pathways, and vascular networks within a living organism. Animal experiments were conducted on six-week-old female C57BL/6 NRj mice (Janvier Labs) in accordance with European Directive 2010/63/EU and its transposition into French law (Decree no. 2013-118). The study was approved by a local ethics committee and carried out at the CEA-SHFJ imaging platform (authorization D91-471-105). Mice were housed under standard conditions: in microisolator polycarbonate cages with aspen wood bedding, five animals per cage, at a controlled room temperature of 22 °C and 40% humidity, under a 12-hour light/dark cycle. Food and water were provided *ad libitum*. During imaging, anesthesia was induced and maintained with isoflurane (2% to 2.5%) under an oxygen flow. To prevent hypothermia, animals were placed on a heated platform that maintained their body temperature between 36 °C and 37 °C. The animals were humanely euthanized *via* cervical dislocation under deep anesthesia induced by 4% isoflurane. This method ensured rapid and ethically compliant termination, minimizing any potential suffering.

Author contributions

Conception and design: C. C., A. N., and C. T.; analysis and interpretation of the data: C. C., S. T., M. R., L. J., D. K., B. J., E. S., B. L., S. M., N. T., A. N., and C. T.; drafting of the paper: C. C., M. R., N. T., A. N., and C. T.; critical revision for intellectual content: C. C., S. T., M. R., L. J., D. K., B. J., E. S., B. L., S. M., N. T., A. N., and C.T.; final approval of the version to be published: C. C., S. T., M. R., L. J., D. K., B. J., E. S., B. L., S. M., N. T., A. N., and C. T. All authors agree to be accountable for all aspects of the work.

Conflicts of interest

A. N. and B. L. are the stockholders of a company developing a FUS device for BBB opening in patients. Other authors have no relevant financial or non-financial interests to disclose.

Data availability

All data supporting this study are included in the article and SI. Supplementary information is available. See DOI: https://doi.org/10.1039/d5pm00088b.

Acknowledgements

We gratefully acknowledge the financial support from ITMO Cancer-Aviesan, provided through INSERM for the IM2FUS project and from INCA – High Risk High Gain for the Keystone project. This work was conducted using an imaging platform that is part of the France Life Imaging network (grant ANR-11-INBS-0006).

References

1 D. H. Upton, C. Ung, S. M. George, M. Tsoli, M. Kavallaris and D. S. Ziegler, Challenges and opportunities to penetrate the blood-brain barrier for brain cancer therapy, *Theranostics*, 2022, **12**, 4734–4752.
2 M. Pinkiewicz, M. Pinkiewicz, J. Walecki, A. Zaczyński and M. Zawadzki, Breaking Barriers in Neuro-Oncology: A Scoping Literature Review on Invasive and Non-Invasive Techniques for Blood-Brain Barrier Disruption, *Cancers*, 2024, **16**, 236.
3 C. D. Arvanitis, G. B. Ferraro and R. K. Jain, The blood-brain barrier and blood-tumour barrier in brain tumours and metastases, *Nat. Rev. Cancer*, 2020, **20**, 26–41.
4 C. Bérard, C. Truillet, B. Larrat, *et al.*, Anticancer drug delivery by focused ultrasound-mediated blood-brain/tumor barrier disruption for glioma therapy: From bench-side to bedside, *Pharmacol. Ther.*, 2023, **250**, 108518.
5 O. Cohen-Inbar, Z. Xu and J. P. Sheehan, Focused ultrasound-aided immunomodulation in glioblastoma multiforme: a therapeutic concept, *J. Ther. Ultrasound*, 2016, **4**, 2.
6 T. Mainprize, N. Lipsman, Y. Huang, *et al.*, Blood-Brain Barrier Opening in Primary Brain Tumors with Non-invasive MR-Guided Focused Ultrasound: A Clinical Safety and Feasibility Study, *Sci. Rep.*, 2019, **9**, 321.
7 B. Marty, B. Larrat, M. Van Landeghem, *et al.*, Dynamic study of blood-brain barrier closure after its disruption using ultrasound: a quantitative analysis, *J. Cereb. Blood Flow Metab.*, 2012, **32**, 1948–1958.
8 C. Chevaleyre, A. Novell, N. Tournier, *et al.*, Efficient PD-L1 imaging of murine glioblastoma with FUS-aided immunoPET by leveraging FcRn-antibody interaction, *Theranostics*, 2023, **13**, 5584–5596.
9 V. L. Tran, A. Novell, N. Tournier, *et al.*, Impact of blood-brain barrier permeabilization induced by ultrasound associated to microbubbles on the brain delivery and kinetics of cetuximab: An immunoPET study using 89Zr-cetuximab, *J. Controlled Release*, 2020, **328**, 304–312.

10 M. Richard, S. Specklin, M. Roche, F. Hinnen and B. Kuhnast, Original synthesis of radiolabeling precursors for batch and on resin one-step/late-stage radiofluorination of peptides, *Chem. Commun.*, 2020, **56**, 2507–2510.
11 G. Hugon, S. Goutal, A. Dauba, *et al.*, [18F]2-Fluoro-2-deoxy-sorbitol PET Imaging for Quantitative Monitoring of Enhanced Blood-Brain Barrier Permeability Induced by Focused Ultrasound, *Pharmaceutics*, 2021, **13**, 1752.
12 E. Porret, D. Kereselidze, A. Dauba, *et al.*, Refining the delivery and therapeutic efficacy of cetuximab using focused ultrasound in a mouse model of glioblastoma: An 89Zr-cetuximab immunoPET study, *Eur. J. Pharm. Biopharm.*, 2023, **182**, 141–151.
13 Y. Meng, R. M. Reilly, R. C. Pezo, *et al.*, MR-guided focused ultrasound enhances delivery of trastuzumab to Her2-positive brain metastases, *Sci. Transl. Med.*, 2021, **13**, eabj4011.
14 L. G. Dubois, L. Campanati, C. Righy, *et al.*, Gliomas and the vascular fragility of the blood brain barrier, *Front. Cell. Neurosci.*, 2014, 8.
15 T. A. Arsiwala, K. E. Blethen, C. P. Wolford, *et al.*, Blood-tumor barrier opening by MRI-guided transcranial focused ultrasound in a preclinical breast cancer brain metastasis model improves efficacy of combinatorial chemotherapy, *Front. Oncol.*, 2023, **13**, 1104594.
16 R. Ji, M. E. Karakatsani, M. Burgess, M. Smith, M. F. Murillo and E. E. Konofagou, Cavitation modulated inflammatory response following focused ultrasound blood-brain barrier opening, *J. Controlled Release*, 2021, **337**, 458–471.
17 S. Goutal, A. Novell, S. Leterrier, *et al.*, Imaging the impact of blood-brain barrier disruption induced by focused ultrasound on P-glycoprotein function, *J. Controlled Release*, 2023, **361**, 483–492.
18 K. Pernet-Gallay, P.-H. Jouneau, A. Bertrand, *et al.*, Vascular permeability in the RG2 glioma model can be mediated by macropinocytosis and be independent of the opening of the tight junction, *J. Cereb. Blood Flow Metab.*, 2017, **37**, 1264–1275.
19 B. Gril, D. Wei, A. S. Zimmer, *et al.*, HER2 antibody-drug conjugate controls growth of breast cancer brain metastases in hematogenous xenograft models, with heterogeneous blood–tumor barrier penetration unlinked to a passive marker, *Neuro-Oncology*, 2020, **22**, 1625–1636.
20 L. Santos, J. N. Moreira, A. Abrunhosa and C. Gomes, Brain metastasis: An insight into novel molecular targets for theranostic approaches, *Crit. Rev. Oncol. Hematol.*, 2024, **198**, 104377.